1988

Exact Analytical Representation of Screw Compressor Rotor Geometry

P. J. Singh
Ingersoll-Rand Co.

J. R. Schwartz
Loral Electronic Systems

EXACT ANALYTICAL REPRESENTATION OF SCREW COMPRESSOR ROTOR GEOMETRY

Pawan J. Singh
Ingersoll-Rand Co.
Phillipsburg, N.J.

Jeremy R. Schwartz
Loral Electronic Systems
Yonkers, N.Y.

1. ABSTRACT

Screw compressor rotors' geometry plays a crucial, if not dominant, role in the compressor's design and performance. The rotor profile not only affects performance and torque distribution between the two rotors, but also the axial and radial loads. The helical rotor surfaces are defined by the end profiles and the helical pitch angle. The traditional method to define these surfaces had been the two-dimensional slice approach, with the rotor represented by a combination of a number of cross sections along the rotor length. While practical, this technique requires dealing with a large number of sections to maintain accuracy. This process can be quite cumbersome and time-consuming.

This paper presents a technique to define the rotor surfaces, exactly, in three-dimensional space. The surface boundaries of the closed volume defining a compressor cavity are represented by the male and female rotor surfaces, end sections, and rotor housing. Once the cavity is defined this way, mathematical operations on this definition can yield important parameters, such as cavity volume as a function of rotor rotation, and blow-hole area. This approach eliminates the need for dealing with the problem in a piecemeal fashion and leads to an exact definition.

2. INTRODUCTION

To a large extent, screw compressor performance depends on the definition of rotor geometry. A clear example of this dependence is the switch from symmetrical to asymmetrical rotor profiles in the 1960s, which produced a quantum jump in overall efficiency of the order of 8-10%.

The process of generating and checking the profiles used to be a laborious, time-consuming task until the use of computers tremendously speeded this work in the early 1980s {1,2,3}. With the widespread use of CAD/CAM, the process of rotor geometry definition, cutting tool design, and final rotor machining can be integrated in one step. The access to this revolutionary tool provides a designer with considerable latitude to match compressor design to a particular application to achieve optimal performance. Performance in this context is not only restricted to the thermodynamic efficiency, but also to mechanical aspects, such as bearing and shaft design, which are greatly influenced by the profile dependent loads.

The traditional method of performing computer analysis of a profile geometry is to use the two-dimensional 'slice' approach.

In this method the rotors are cut along the axes in planes parallel to the end-view plane, and each slice is evaluated, using plane geometry principles. These slices are combined by integrating the values calculated along the rotor length. Obviously, the accuracy of this technique depends on the number of slices used in the analysis. While this technique is adequate for most applications, it remains deficient in the following ways:

o Certain geometrical features such as blow-hole, are highly three-dimensional and cannot be adequately represented by the slice method.

o For accurate analysis of certain profiles, the required number of slices could be quite large. In addition, this number is not generally apriori known.

o Each slice requires human judgment, so that complete automation through a computer algorithm is not possible.

Fortunately, although seemingly quite complex, screw compressor geometry can be represented analytically without much difficulty. This is because the cross section at any point along the rotor can be defined by an appropriate rotation of the end profile (Figure 1). The difficulty arises in defining the contact points along the rotors which do not follow any set pattern and are a function of the rotor profiles, and in the definition of the blow-hole. This paper sets up a mathematical representation of the rotor and housing geometry and demonstrates how useful information regarding the cavity volume and other geometrical parameters can be extracted from this analysis.

3. METHODOLOGY

This section outlines the basic framework used in setting up the problem:

o The divergence theorem is used whenever possible to reduce the volume integrals to surface integrals and surface integrals to line integrals.

o The rotor end profiles are defined by a series of points along the profile used in its generation. Similarly, rotor-to-rotor contact lines can be defined by points derived from the profile generation program described in {1}. Also, the rotor profiles can be defined by a closed-form solution, if available. Only one male and one female lobe need to be defined, and the periodicity condition is applied to define other lobes.

o The meshed rotors are assumed to extend infinitely in both directions as shown in Figure 2. The rotor length can be defined by two planes perpendicular to the rotor axes and length L apart. The variation in rotor cavity volume, due to rotation, then can be simulated by translation of the two parallel planes. One can conclude that the rotation of helical rotors is equivalent to traveling along the rotors.

o In its most general form, a rotor cavity is defined by the end plane, contact line, leading and trailing housing cusp lines, and leading and trailing blow-holes. During early suction process and late discharge process, the cavity may involve one or two cusp lines and blow-holes.

o A coordinate grid that covers a rotor surface is provided by arc length measured along a traversal around the rotor profile, up the hills and down the valleys, and by helical lines along the surface. These grids are laid out as rotor surface maps in Figure 2. Arc length around a profile, p, is laid out horizontally, while helical lines along the surface become vertical grid lines. The oblique curvilinear contours are the projections, on the respective surfaces, of the contact line in space, along which each rotor cuts across the surface of the other. These may be plotted rather directly from given data defining the rotor profiles and the rotor rotation angle required to bring each pair of profile points into contact. The horizontal coordinate, arc length, is accumulated increment by increment around the profile from the profile data alone. The vertical coordinate may be taken numerically equal to its corresponding rotor rotation angle, since the profile section oriented to make contact is a proportionate distance away axially.

The accented vertical lines in Figure 2 represent helical lines along the crests of the rotors, where the housing would be touched, but for clearance. The intersection of an end face with a rotor surface is a horizontal line. Between the upper ends of the vertical crest lines and the upper contact line projection is a considerable interval that borders a hole between rotor lobes in the vicinity of the housing cusp line that meets the inlet port at the inlet end face. The interval between the lower ends of the vertical crest lines and the lower contact line projection is quite small. It borders the blow-hole between adjacent compression chambers in the vicinity of the housing cusp line that meets the discharge port at the discharge end face. This small blow-hole is of concern in leakage calculations. In the volume calculation, it provides a small part of the surface bounding the compression chamber.

o Once the rotor surfaces have been defined, definition of other surfaces, such as housing and end planes, is relatively simple. The integrals around these surfaces are then used to calculate various design parameters, such as cavity volume as a function of rotation or blow-hole area. The only input variables for these calculations are profile definitions, number of male and female rotor lobes, wrap, angle and rotor length.

4. ANALYSIS

The analytical method can best be illustrated by its use to calculate cavity volume. Figure 3 defines the global coordinate system (x_i, $i = 1,2,3$) and local coordinate systems with origins at male rotor axis x_i^M and female rotor axis x_i^F respectively. For the sake of compactness, vector and tensor notations are used here extensively.

If V is the volume of the cavity under consideration and S is the closed surface bounding it,

$$V = \frac{1}{3} \oint_V \nabla . \vec{r} \, dV = \frac{1}{3} \oint \vec{n} . \vec{r} \, dS \qquad (1)$$

where $\vec{r}$ is the position vector from a common origin. The surface S consists of several components defined as below,

$$S = S_R \cup S_H \cup S_E \cup S_{BH} \qquad (2)$$

Where

S_R = Combination of relevant male rotor surface (S_{MR}) and female rotor surface (S_{FR})

S_H = Combination of relevant male rotor housing (S_{MH}) and female rotor housing (S_{FH})

S_E = Combination of relevant male end rotor plane surface (S_{ME}) and female rotor end plane surface (S_{FE})

S_{BH} = Combination of leading blow-hole surface (S_{LBH}) and trailing blow-hole surface (S_{TBH})

The volume integral then decomposes as follows:

$$3V = I_R + I_H + I_E + I_{BH} \tag{3}$$

where $I_R = \int_{S_R} \vec{n}.\vec{r}\, ds = \int_{S_{MR}} \vec{n}.\vec{r}\, ds + \int_{S_{FR}} \vec{n}.\vec{r}\, ds$, etc. (4)

Let us now consider each integral individually, starting with male rotor integral I_{MR}, involving surface S_{MR}, (Figure 4).

$$I_{MR} = \int_{S_{MR}} \vec{n}.\vec{r}\, ds \tag{5}$$

Changing origin to male rotor axis (Figure 3), we get,

$$\vec{r} = \vec{r}_M + \vec{C}_M \tag{6}$$

Where $\vec{r}_M$ is the position vector in the new coordinate system and $\vec{C}_M$ is the position vector of the new origin. Then,

$$I_{MR} = \int_{S_{MR}} \vec{C}_M.\vec{n}\, ds + \int_{S_{MR}} \vec{r}_m.\vec{n}\, ds \tag{7}$$

In Figure 3, let the axial direction x_3 have a sense of a right-handed screw from x_1 to x_2 (i.e. out of paper towards the reader). Also let the reference profile lie in the plane $x_3 = 0$. For integration purposes, it is more convenient to represent the position vector in a parametric form, i.e.,

$$\vec{R}_M(p_M) = \vec{e}_i\, X_i(p_M), \quad i = 1, 2 \tag{8}$$

$$\vec{R}_F(p_F) = \vec{e}_i\, X_i(p_F), \quad i = 1, 2 \tag{9}$$

where p_M, p_F are taken as arc lengths along their respective profiles, increasing in the sense of respective rotations of the rotors, starting from zero at the trailing crest and increasing monotonically to lobe profile arc length at the leading crest (Figure 5). $\vec{e}_i$ are unit vectors in the global or unrotated local coordinate system, $\vec{R}$ is a position vector in the $x_3=0$ plane, and x_i are coordinates of the profile points in this plane. Therefore, as seen in Figure 6,

$$\vec{r}_M = \vec{\Omega}_M.\vec{R}_M + \vec{e}_3\, \zeta_M \theta_M \tag{10}$$

$$\vec{r}_F = \vec{\vec{\Omega}}_F \cdot \vec{R}_F + \vec{e}_3 \zeta_F \theta_F \tag{11}$$

where $\vec{\vec{\Omega}}_M = \vec{\beta}_i \vec{e}_i$, $\vec{\vec{\Omega}}_F = \vec{\gamma}_i \vec{e}_i$, $i = 1, 2$, (12)

$$\vec{\beta}_1 = \vec{e}_1 \cos\theta_M - \vec{e}_2 \sin\theta_M \tag{13}$$

$$\vec{\beta}_2 = \vec{e}_1 \sin\theta_M + \vec{e}_2 \cos\theta_M \tag{14}$$

$$\vec{\gamma}_1 = \vec{e}_1 \cos\theta_F + \vec{e}_2 \sin\theta_F \tag{15}$$

$$\vec{\gamma}_2 = -\vec{e}_1 \sin\theta_F + \vec{e}_2 \cos\theta_F \tag{16}$$

where $\vec{\vec{\Omega}}_M$, $\vec{\vec{\Omega}}_F$ are rotational transformation dyadics or matrices, ζ_M , ζ_F are respective male and female pitch constants ($\zeta_F = \zeta_M n_F / n_M$, n = number of lobes), and θ is the rotation angle in radians ($\theta_M = n_F \theta_F / n_M$).

Now we need to define normal unit vector locally. $\vec{n}$ is directed outward from the volume and, therefore, inward into each rotor. The vector differential area in the direction of normal for the male rotor is given by,

$$\vec{n}\, dS_M = \left(\vec{r}_{\theta_M} d\theta_M\right) \times \left(\vec{r}_{p_M} dp_M\right) \tag{17}$$

where $\vec{r}_{\theta_M} = \frac{\partial \vec{r}_M}{\partial \theta_M}$ and $\vec{r}_{p_M} = \frac{\partial \vec{r}_M}{\partial p_M}$ are tangential vectors in the θ_M and p_M directions respectively.

Substituting (17) in (7),

$$I_{MR} = \int_{S_{MR}} \vec{C}_M \cdot \left(\vec{r}_{\theta_M} d\theta_M\right) \times \left(\vec{r}_{p_M} dp_M\right) + \int_{S_{MR}} \vec{r}_M \cdot \left(\vec{r}_{\theta_M} d\theta_M\right) \times \left(\vec{r}_{p_M} dp_M\right) \tag{18}$$

From vector calculus, it can be shown that,

$$\left(\vec{r}_{p_M} dp_M\right) \times \left(\vec{r}_{\theta_M} d\theta_M\right) = -\left[\vec{e}_3 d\vec{R}_M \cdot \vec{R}_M + \zeta_M \vec{e}_3 \times \left(\vec{\vec{\Omega}}_M \cdot d\vec{R}_M\right)\right] d\theta_M \tag{19}$$

Therefore, (18) becomes,

$$I_{MR} = \int_{S_{MR}} \vec{C}_M \cdot \left[\vec{e}_3 d\vec{R}_M \cdot \vec{R}_M + \zeta_M \vec{e}_3 \times \left(\vec{\vec{\Omega}}_M \cdot d\vec{R}_M\right)\right] d\theta_M$$

$$+\int_{S_{MR}} \rho_M \left[\theta_M \, d\vec{R}_M \cdot \vec{R}_M + \vec{e}_3 \cdot d\vec{R}_M \times \vec{R}_M \right] d\theta_M \qquad (20)$$

Next we want to transform surface integrals into line integrals by carrying out the integration with respect to θ_M on the (ρ_M, θ_M) plane.

For example, for a function F (ρ,θ), integration along surface S (Figure 7) can be reduced to integration around boundary of S by noting,

$$\iint_S \frac{\partial F(\rho,\theta)}{\partial \theta} \, d\theta \, d\rho = \int_a^b \left[F\left(\rho, \theta_2(\rho)\right) - F\left(\rho, \theta_1(\rho)\right) \right] d\rho$$

$$= -\int_a^b F\left(\rho, \theta_2(\rho)\right) d\rho - \int_a^b F\left(\rho, \theta_1(\rho)\right) d\rho$$

$$= -\oint_C F\left(\rho, \theta(\rho)\right) d\rho \qquad (21)$$

with C running counterclockwise.

Using (21) and noting that

$$\vec{e}_3 \times \left(\vec{\vec{\Omega}}_M \cdot d\vec{R}_M \right) = -\frac{\partial}{\partial \theta_M} \left(\vec{\vec{\Omega}}_M \cdot d\vec{R}_M \right) \qquad (22)$$

(20) reduces to,

$$I_{MR} = \oint_{C_{MR}} \rho_M \vec{C}_N \cdot \vec{\vec{\Omega}}_M \cdot d\vec{R}_M - \oint_{C_{MR}} \rho_M \left(\tfrac{1}{2} \theta_M^2 \, d\vec{R}_M \cdot \vec{R}_M + \theta_M \vec{e}_3 \cdot d\vec{R}_M \times \vec{R}_M \right) \qquad (23)$$

C_{MR} is the boundary of surface S_{MR} in the p- θ plane (Figure 6).

Equation (23) now can be integrated using only the profile information obtained from the profile generation programs{1}.

Detailed derivation of each integral in (2) is not possible here, due to limitations on the paper's length. However, such derivation is given in {5}. In each case, the transformation of integrals from x_i coordinate system to (ρ, θ) system and the use of vector identities leads to line integrals which can then be easily programmed on a computer.

5. BLOW-HOLE AREA

The definition of blow-hole is required in the cavity volume calculations since one or both (leading and trailing) blow-holes are used in the analysis to close the cavity. Each blow-hole is bounded by a curvilinear triangle. One side of this triangle is the housing cusp between leading and trailing crests of the two rotors. The other two sides are paths from the crest-cusp intersections, along the respective rotor surfaces to a common point where the two rotors make contact. It will make sense that the correct choice of contact point for the third vortex is

the one that minimizes the amplitude of the vector area of the blow-hole, defined as,

$$\vec{S}_{BH} = \int_{S_{BH}} \vec{n}\, dS \tag{24}$$

In consequence of an integral transformation,

$$\vec{S}_{BH} = \frac{1}{2} \oint_{C_{BH}} \vec{r} \times d\vec{r} \tag{25}$$

where C_{BH} is the closed boundary of S_{BH} traversed in the sense of a right-handed screw with respect to the sense of the unit normal vector $\vec{n}$ to surface S_{BH}.

Each curvilinear blow-hole boundary, lying on a rotor surface, cuts across some of the helical lines defined by given profile arrays, as it passes from a crest-cusp intersection to the chosen contact points between rotors. The third vertex of the blow-hole is not a priori defined for all cases. Since this vertex must be a contact point, the computer program used to calculate blow-hole area selects a number of contact points in the expected region, calculates blow-hole area one by one, and selects the minimum as the correct area.

The integral for the vector area, S_{BH}, may be decomposed of as,

$$2\,\vec{S}_{BH} = \vec{I}_C + \vec{I}_M + \vec{I}_F \tag{26}$$

where

$$\vec{I}_C = \int_{C_C} \vec{r} \times d\vec{r}\,, \quad \vec{I}_M = \int_{C_M} \vec{r} \times d\vec{r}\,, \quad \vec{I}_F = \int_{C_F} \vec{r} \times d\vec{r} \tag{27}$$

and C_C, C_M, C_F, are relevant parts of the curves along housing cusp, male and female rotors respectively.

We will just consider one of the integrals here to show that they can be reduced to either closed-form solutions, or to simpler integrals involving geometric parameters that are solvable by numerical integration. The simplest integral is I_C along the housing cusp.

$$I_C = \int_{C_C} \vec{r} \times d\vec{r}\,, \quad \vec{r} = -\vec{e}_2 h + \vec{e}_3 x_3, \quad \zeta_F \theta_{FD} \le x_3 \le \zeta_M \theta_{MD} \tag{28}$$

where h is the distance of cusp line from the (x_1, x_3) plane, and θ_{FD} and θ_{MD} are the respective female and male rotor rotation angles required to translate the cross-sectional profiles from $x_3=0$ plane to those constituting the blow-hole. Then,

$$\vec{r} \times d\vec{r} = -\vec{e}_1 h\, dx_3 \tag{29}$$

and

$$I_C = \int_{\zeta_F \theta_{FD}}^{\zeta_M \theta_{MD}} -\vec{e}_1 h\, dx_3 = -\vec{e}_1 h \left(\zeta_F \theta_{FD} - \zeta_M \theta_{MD}\right) \tag{30}$$

The axial and cross-sectional components of I_C are,

$$\vec{e}_3 \cdot \vec{I}_c = 0 \tag{31}$$

$$\vec{e}_3 \times \vec{I}_c = \vec{e}_2 h \left(\zeta_F \theta_{FD} - \zeta_M \theta_{MD}\right) \tag{32}$$

Other integrals, I_M and I_F, can also be further reduced but with much greater complexity. Details of these derivations are given in {5}.

We are primarily interested in the blow-hole leakage area, i.e., area normal to the flow direction. From the blow-hole configuration, we can safely assume that the nominal leakage flow direction is along the female rotor flank near the crest. Thus we need to determine the blow-hole surface, normal to the tangent to the trailing female crest line, evaluated at the cusp-crest intersection that is one corner of the blow-hole. The sense of the tangent will be taken along a helix backward toward the inlet.
The tangent to a helix at the discharge side cusp intersection, forward toward the discharge, is,

$$\frac{\partial \vec{r}}{\partial \theta_F} = -\vec{e}_2 C_F + \vec{e}_1 h + \vec{e}_3 \zeta_F \tag{33}$$

where $C_F = (C^2+R_F^2-R_M^2)/2C$, C is the center distance between the two rotors, and R_M and R_F are male and female rotor radii respectively.

The desired unit tangent vector, backward toward the inlet, is defined by,

$$T = -\frac{\partial \vec{r}}{\partial \theta_F} \Big/ \left|\frac{\partial \vec{r}}{\partial \theta_F}\right| = \left(-\vec{e}_1 h + \vec{e}_2 C_F - \vec{e}_3 \zeta_F\right) \Big/ \left(h^2 + C_F^2 + \zeta_F^2\right)^{1/2} \tag{34}$$

The desired projection S_T of the blow-hole area S_{BH}, normal to the nominal direction of the leakage flow, is,

$$S_T = \vec{S}_{BH} \cdot \vec{T} = T_1 S_1 + T_2 S_2 + T_3 S_3 \tag{35}$$

where S_i, i = 1 to 3 are the components of the blow-hole vector area.

6. DISCUSSION

What has been presented here is a framework for analytical evaluation of main geometric characteristics of screw compressor air-end design. Along with the profile generation routines, this work constitutes a comprehensive basis for computer-based rotor profile design and evaluation, inlet and discharge port design, and evaluation of compressor performance. This analysis is independent of profile shape and its properties, and is designed to be universal in nature. Although the mathematical complexity seems daunting at first glance, once programmed in a computer, this complexity becomes transparent to the user.

New developments in computer-aided design (CAD), solids modeling, high-resolution graphics, and the availability of user-friendly software to model and visualize complex geometries on a computer screen eliminate the need for deriving

and programming mathematical relationships presented in this paper. Many of these relationships are already included in the software in the form of algorithms. Once these mathematical barriers are overcome, the relevance of this paper to a compressor designer becomes more apparent. The concepts and ideas presented here can now be applied to CAD generated rotor and housing surfaces to compute cavity volume, blow-hole area, and discharge part shape.

7. CONCLUSIONS

It has been shown that the screw compressor geometry, while seemingly complex, is amenable to complete analytical representation. This mathematical formulation can then be manipulated to yield several quantities of direct interest to a compressor designer such as cavity volume and its variation with rotor rotation, blow-hole area, etc. The volume and surface integrals can be reduced to closed-form solutions or simplified integrands that can be numerically solved on a computer. This scheme, along with a few other computer programs {1}, allows completely automated analysis from profile generation to performance prediction for any given profile in one package. The senior author's company uses some of these programs on a routine basis to calculate profile characteristics like blow-hole area which are otherwise difficult to compute accurately. In concert with current advances in CAD and solids modeling, underlying themes presented here can now be effectively utilized without the need for detailed derivation or programming of mathematical equations.

8. ACKNOWLEDGMENTS

The authors are grateful in Ingersoll-Rand management for the permission to publish this paper. Special thanks go to Mr. Alec Sherrill of Portable Compressor Division and Mr. Art Jamison of Rotary Compressor Division for sponsoring this work at Ingersoll-Rand Research Center where both authors worked during conduct of this research program.

9. REFERENCES

1. Singh, P. J. and Onuschak, A. D., "A Comprehensive, Computerized Method For Twin Screw Rotor Profile Generation & Analysis," International Compressor Engineering Conference at Purdue, 1984.

2. Singh, P. J. and Bowman, J. L., "Effect of Design Parameters on Oil-Flooded Screw Compressor Performance," Proceedings of the 1986 International Compressor Engineering Conference at Purdue, 1986.

3. Fujiwara, M., Kasuya, K., Matsunaga, T., and Watanabe, M., "Computer Modeling For Performance Analysis of Rotor Screw Compressor," Proceedings of the 1984 International Compressor Engineering Conference at Purdue, 1984.

4. Sjoholm, L., "Different Operational Modes for Refrigeration Twin-Screw Compressors, "Proceedings of the 1986 International Compressor Engineering Conference at Purdue, 1986.

5. Schwartz, J., "Screw Compressor Performance - Foundation of the Computer Program for the Chamber Volume and Blowhole Area," Ingersoll-Rand Research, Inc., Technical Note No. TN-479, 1980.

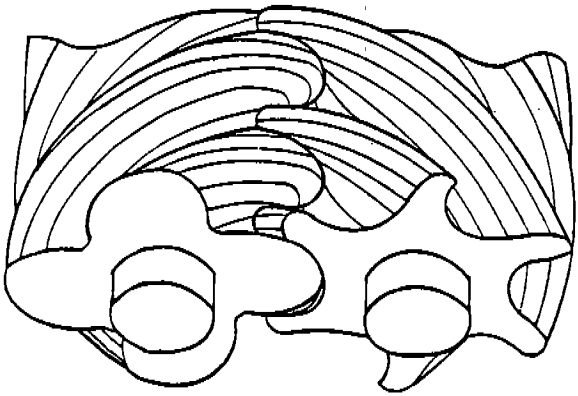

FIGURE 1: MESHED ROTORS IN A TWIN-SCREW COMPRESSOR ADAPTED FROM [4].

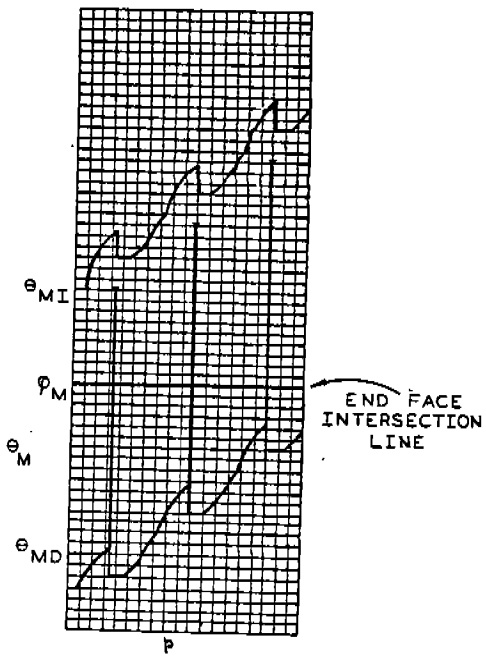

FIGURE 2A: REPRESENTATION OF MALE ROTOR IN THE TRANSFORMED (φ ,θ) PLANE. DARK VERTICAL LINES REPRESENT ROTOR LOBE CRESTS.

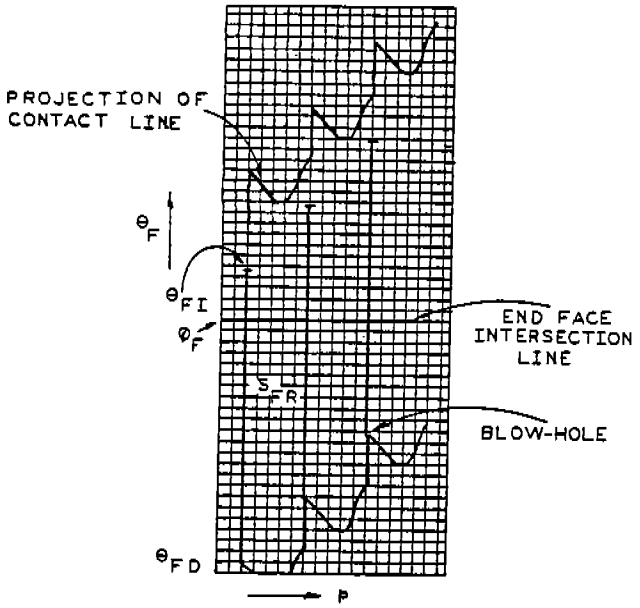

FIGURE 2B: REPRESENTATION OF FEMALE ROTOR IN THE TRANSFORMED (ϕ ,θ) PLANE. DARK VERTICAL LINES REPRESENT ROTOR LOBE CRESTS.

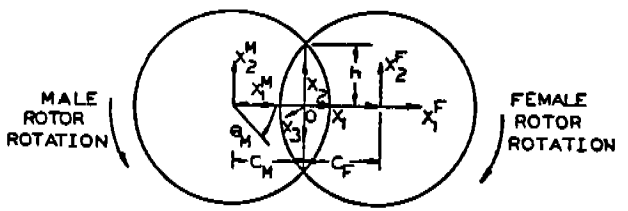

FIGURE 3: DEFINITION OF VARIOUS COORDINATE SYSTEMS USED IN THE ANALYSIS.

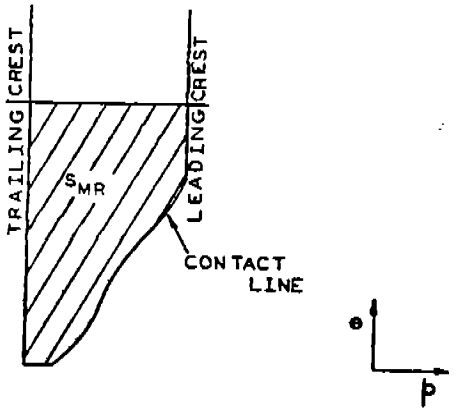

FIGURE 4: DEFINITION OF SURFACE S_{MR} IN THE (þ -θ) PLANE.

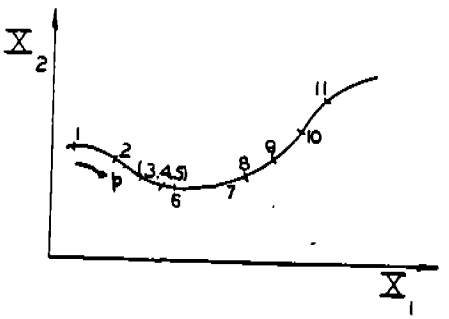

FIGURE 5: DEFINITION OF PARAMETER Þ , ARC LENGTH ALONG THE ROTOR PROFILE.

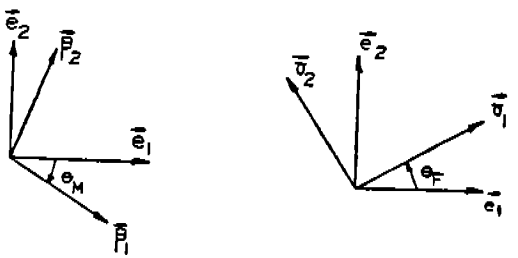

FIGURE 6: COORDINATE ROTATION CONVENTION USED IN THE ANALYSIS.

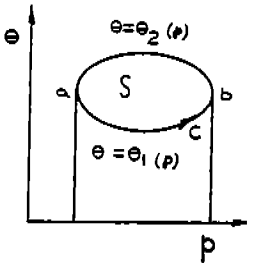

FIGURE 7: DEFINITION OF SURFACE S AND BOUNDARY C IN SURFACE TO LINE TRANSFORMATION.